Inorg. Chem. **2006**, *45*, 4602–4609

The Metal–NO Interaction in the Redox Systems $[Cl_5Os(NO)]^{n-}$, $n = 1–3$, and *cis*-$[(bpy)_2ClOs(NO)]^{2+/+}$: Calculations, Structural, Electrochemical, and Spectroscopic Results

Priti Singh,[†] Biprajit Sarkar,[†] Monika Sieger,[†] Mark Niemeyer,[†] Jan Fiedler,[‡] Stanislav Záliš,*[,‡] and Wolfgang Kaim*[,†]

Institut für Anorganische Chemie, Universität Stuttgart, Pfaffenwaldring 55, D-70550 Stuttgart, Germany, and J. Heyrovsky Institute of Physical Chemistry, Academy of Sciences of the Czech Republic, Dolejškova 3, CZ-18223 Prague, Czech Republic

Received October 12, 2005

Experimental and computational results for the two-step redox system $[Cl_5Os(NO)]^{n-}$ ($n = 1–3$) are reported and discussed in comparison to the related one-step redox systems $[Cl_5Ru(NO)]^{n-}$ and $[Cl_5Ir(NO)]^{n-}$ ($n = 1, 2$). The osmium system exhibits remarkably low oxidation and reduction potentials. The structure of the precursor $(PPh_4)_2[Cl_5Os(NO)]$ is established as an $\{MNO\}^6$ species with almost linear OsNO arrangement at 178.1°. Density-functional theory (DFT) calculations confirm this result, and a comparison of structures calculated for several oxidation states reveals an increased labilization of the trans-positioned M–Cl bond on reduction in the order M = Ir < Os < Ru. Accordingly, the intact reduced form $[Cl_5Os(NO)]^{3-}$ could not be observed in fluid solution even on electrolysis at –70 °C in *n*-butyronitrile solution, as confirmed both by DFT calculations and by comparison with the electron paramagnetic resonance and infrared spectroelectrochemically characterized redox pairs *cis*-$[(bpy)_2ClOs(NO)]^{2+/+}$ and $[(CN)_5Os(NO)]^{2-/3-}$. The DFT calculations indicate that the oxidation of $[Cl_5Os(NO)]^{2-}$ occurs largely on the metal, the highest occupied molecular orbital (HOMO) of the precursor being composed of Os 5d (58%) and Cl_{eq} 3p orbitals (41%). As for the related $[(CN)_5Os(NO)]^{2-}$, the reduction is largely NO centered, the lowest unoccupied molecular orbital (LUMO) of $[Cl_5Os(NO)]^{2-}$ has 61% π^*(NO) character with significant 5d Os contributions (34%). A rather large degree of metal–NO back-donation is estimated to occur in the $\{OsNO\}^7$ configuration of $[Cl_5Os(NO)]^{3-}$ which leads to an unusual low value of 1513 cm^{-1} calculated for ν(NO), signifying contributions from an $Os^{III}(NO^-)$ formulation. Detailed analyses of the conformational dependence of the *g* anisotropy suggest that the different reduced species reported previously for $[Cl_5Os(NO)]^{3-}$ in AgCl host lattices may be distinct in terms of eclipsed or staggered conformations of the bent $NO^•$ axial ligand relative to the $Os^{II}Cl_4$ equatorial plane. The staggered form is calculated to be more stable by 105 cm^{-1}. The weak absorptions of $[Cl_5Os(NO)]^{2-}$ at 573, 495, and 437 nm are assigned as MLCT/LLCT transitions to the doubly degenerate π^*(NO) LUMO. The oxidized form $[Cl_5Os(NO)]^-$ contains Os^{III} in an $\{OsNO\}^5$ configuration with a spin density of 0.711 on Os. In all three states of $[Cl_5Os(NO)]^{n-}$, the N bonded form is vastly preferred over the NO-side-on bonded alternative.

Introduction

The discovery[1a] of various essential physiological functions of "NO" during the last 2 decades not only has spawned an explosive growth in the pertinent medical and biosciences literature[1] but also has rekindled the interest in the coordination chemistry of the noninnocent nitrosyl ligand[2] because many processes of NO formation, release, and binding involve metal/NO interactions. The NO ligand may bind as nitrosyl cation NO^+, as neutral nitric oxide radical $NO^•$, or as nitroxyl anion NO^-.[2]

* To whom correspondence should be addressed. E-mail: kaim@iac.uni-stuttgart.de (W.K.); stanislav.zalis@jh-inst.cas.dz (S.Z.).
[†] Universität Stuttgart.
[‡] Academy of Sciences of the Czech Republic.

(1) (a) Murad, F. *Angew. Chem., Int. Ed. Engl.* **1999**, *38*, 1856. (b) Feelisch, M., Stamler, J. S., Eds. *Methods in Nitric Oxide Research*; Wiley: Chichester, U.K., 1996. (c) Wang, P. G.; Xian, M.; Tang, X.; Wu, X.; Wen, Z.; Cai, T.; Janczuk, A. *Chem. Rev.* **2002**, *102*, 1091. (d) Hrabie, J. A.; Keefer, L. K. *Chem. Rev.* **2002**, *102*, 1135. (e) Wang, P. G., Cai, T. B., Taniguchi, N., Eds. *Nitric Oxide Donors*; Wiley-VCH: Weinheim, Germany, 2005.

10.1021/ic0517669 CCC: $33.50
Published on Web 05/11/2006

In addition to the general biological significance[1,3] and the pharmaceutical potential, the catalytic functions of nitrosyl complexes as intermediates in technical processes[4] and the photochemistry with respect to metastable nonconventional M(NO) binding[5] are also of current interest. As a further application-oriented example, the systems $[Cl_5M(NO)]^{2-}$, M = Ru, Os, have been proposed[6] as image contrast enhancing photoelectron trapping dopants in AgCl where the reduced forms $[Cl_5M(NO)]^{3-}$ could be characterized by a detailed electron paramagnetic resonance (EPR) study.[6]

In contrast to numerous studies on iron nitrosyl complexes[2,7] and still many reports on ruthenium compounds containing the $NO^+/NO^\bullet$ ligand,[2,8] there have been far fewer investigations for nitrosylosmium species.[9−13] Porphyrin[10] and bipyridine complexes[11] and their electrochemistry are known, and for simple systems such as $[X_5Os(NO)]^{2-}$ (X = Cl, Br, I)[12] and $[(CN)_5Os(NO)]^{2-}$ some neighboring redox states could be characterized by EPR spectroscopy.[6,12a,13]

Following a previous study[14] on the $[Cl_5Ru(NO)]^{n-}$ and $[Cl_5Ir(NO)]^{n-}$ redox pairs (n = 1, 2), we now report experimental and computational results for the potential two-step redox system $[Cl_5Os(NO)]^{n-}$ (n = 1−3) and for the reference *cis*-$[(bpy)_2ClOs(NO)]^{2+/+}$, the homologue of the well studied pair *cis*-$[(bpy)_2ClRu(NO)]^{2+/+}$.[8a,15] As will become apparent by the results described, the absence of a chloride ligand in trans position to NO enhances the stability of the reduced form and allowed us to use this system as a reference for EPR and IR studies. The following points will be addressed for $[Cl_5Os(NO)]^{n-}$ in comparison to the ruthenium and iridium systems: (i) the wide variation of redox potentials, (ii) structural aspects in correlation with electrochemical reactivity, (iii) the site of electron transfer as evident from low-temperature EPR and IR spectroelectrochemistry, (iv) the spin distribution in paramagnetic states as calculated and reflected by **g** tensor anisotropy, (v) the nature of excited states as calculated and as deduced from spectroscopy, (vi) configurational aspects of NO^+ binding to osmium(III) (N vs O or η^2-NO coordination), and (vii) conformational aspects of $NO^\bullet$ binding to osmium(II) (eclipsed vs staggered arrangement)[7g,8a,14] in relation to solution and solid-state matrix EPR studies.[6]

Complementing the rapidly increasing work on the potentially useful nitrosylruthenium compounds[8] by research on osmium analogues draws on the established differences between the two metals, that is, on the preference for higher oxidation states and on stronger π back-donation from lower oxidation states as well as on the much higher spin−orbit coupling constant of the heavier homologue. In view of the remarkably invariant EPR characteristics of the $\{RuNO\}^7$ configuration,[8a] it is also of interest to study more osmium systems and to interpret the results using recent DFT approaches. Assigning oxidation states, if only approximate, may be important in estimating and understanding the properties and reactivities of nitrosyl complexes.

Experimental Section

Instrumentation and Procedures. EPR spectra in the X band were recorded with a Bruker System ESP 300 equipped with a Bruker ER035M gaussmeter and a HP 5350B microwave counter. IR spectra were obtained using a Perkin-Elmer 1760 X FTIR instrument. UV−vis−NIR absorption spectra were recorded on a J&M TIDAS spectrophotometer. Cyclic voltammetry was carried out in 0.1 M Bu_4NPF_6 solutions using a three-electrode configuration (glassy-carbon working electrode, Pt counter electrode, Ag/AgCl reference) and a PAR 273 potentiostat and function generator.

(2) (a) McCleverty, J. A. *Chem. Rev.* **2004**, *104*, 403. (b) Enemark, J. H.; Feltham, R. D. *Coord. Chem. Rev.* **1974**, *13*, 339. (c) Westcott, B. L.; Enemark, J. L. In *Inorganic Electronic Structure and Spectroscopy*; Solomon, E. I., Lever, A. B. P., Eds.; Wiley: New York, 1999; Vol. 2, p 403.

(3) (a) Tocheva, E. I.; Rosell, F. I.; Mauk, A. G.; Murphy, M. E. P. *Science* **2004**, *304*, 867. (b) Aboelella, N. W.; Reynolds, A. M.; Tolman, W. B. *Science* **2004**, *304*, 836.

(4) (a) Iwamoto, M.; Hamada, H. *Catal. Today* **1991**, *10*, 57. (b) Groothaert, M. H.; van Bokhoven, J. A.; Battiston, A. A.; Weckhuysen, B. M.; Schoonheydt, R. A. *J. Am. Chem. Soc.* **2003**, *125*, 7629.

(5) Coppens, P.; Novozhilova, I.; Kovalevsky, A. *Chem. Rev.* **2002**, *102*, 861.

(6) (a) Eachus, R. S.; Baetzold, R. C.; Pawlik, T. D.; Poluektov, O. G.; Schmidt, J. *Phys. Rev. B: Condens. Matter Mater. Phys.* **1999**, *59*, 8560. (b) Eachus, R. S.; Pawlik, T. D.; Baetzold, R. C. *J. Phys.: Condens. Matter* **2000**, *12*, 8893.

(7) (a) Ford, P. C.; Lorkovic, I. M. *Chem. Rev.* **2002**, *102*, 993. (b) Karidi, K.; Garoufis, A.; Tsipis, A.; Hadjiliadis, N.; den Dulk, H.; Reedijk, J. *J. Chem. Soc., Dalton Trans.* **2005**, 1176. (c) Praneeeth, V. K. K.; Neese, F.; Lehnert, N. *Inorg. Chem.* **2005**, *44*, 2570. (d) Rovira, C.; Kunc, K.; Hutter, J.; Ballone, P.; Parrinello, M. *J. Phys. Chem. A* **1997**, *101*, 8914. (e) Scheidt, W. R.; Ellison, M. K. *Acc. Chem. Res.* **1999**, *32*, 350. (f) Ghosh, A. *Acc. Chem. Res.* **2005**, *38*, 943. (g) Patchkovskii, S.; Ziegler, T. *Inorg. Chem.* **2000**, *39*, 5354.

(8) (a) Frantz, S.; Sarkar, B.; Sieger, M.; Kaim, W.; Roncaroli, F.; Olabe, J. A.; Zalis, S. *Eur. J. Inorg. Chem.* **2004**, 2902 and literature cited. (b) Sarkar, S.; Sarkar, B.; Chanda, N.; Kar, S.; Mobin, S. M.; Fiedler, J.; Kaim, W.; Lahiri, G. K. *Inorg. Chem.* **2005**, *44*, 6092. (c) Kadish, K. M.; Adamian, V. A.; Van Caemelbecke, E.; Tan, Z.; Tagliatesta, P.; Bianco, P.; Boschi, T.; Yi, G.-B.; Khan, M. A.; Richter-Addo, G. B. *Inorg. Chem.* **1996**, *35*, 1343. (d) Graça Zanichelli, P.; Miotto, A. M.; Estrela, H. F. G.; Rocha Soares, F.; Grassi-Kassisse, D. M.; Spadari-Bratfisch, R. C.; Castellano, E. E.; Roncaroli, F.; Parise, A. R.; Olabe, J. A.; de Brito, A. R. M. S.; Wagner Franco, D. *Inorg. Biochem.* **2004**, *98*, 1921. (e) Tfouni, E.; Queiroz Ferreira, K.; Gorzoni Doro, F.; Santana da Silva, R.; Novais da Rocha, Z. *Coord. Chem. Rev.* **2005**, *249*, 405. (f) Ford, P. C.; Laverman, L. E. *Coord. Chem. Rev.* **2005**, 249, 391.

(9) Ooyama, D.; Nagao, N.; Nagao, H.; Sugimoto, Y.; Howell, F. S.; Mukaida, M. *Inorg. Chim. Acta* **1997**, *261*, 45 and literature cited.

(10) (a) Leal, F. A.; Lorkovic, I. M.; Ford, P. C.; Lee, J.; Chen, L.; Torres, L.; Khan, M. A.; Richter-Addo, G. B. *Can. J. Chem.* **2003**, *81*, 872. (b) Carter, S. M.; Lee, J.; Hixson, C. A.; Powell, D. R.; Wheeler, R. A.; Shaw, M. J.; Richter-Addo, G. B. *J. Chem. Soc., Dalton Trans.* **2006**, 1338.

(11) Pipes, D. W.; Meyer, T. J. *Inorg. Chem.* **1984**, *23*, 2466.

(12) (a) Bhattacharyya, B.; Saha, A. M.; Ghosh, P. N.; Mukherjee, M.; Mukherjee, A. K. *J. Chem. Soc., Dalton Trans.* **1991**, 501. (b) Bobkova, E. Y.; Borkovskii, N. B.; Svetlov, A. A.; Novitskii, G. G. *Zh. Neorg. Khim.* **1994**, *39*, 830; *Chem. Abstr. 121*, 190175. (c) Svetlov, A. A.; Kanishcheva, A. S.; Bobkova, E. Y.; Sinitsyn, M. N.; Mikhailov, Y. N. *Zh. Neorg. Khim.* **1991**, *36*, 2834; *Chem. Abstr. 116*, 48167. (d) Bobkova, E. Y.; Svetlov, A. A.; Rogalevich, N. L.; Novitskii, G. G.; Borkovskii, N. B. *Zh. Neorg. Khim.* **1990**, *35*, 981; *Chem. Abstr. 113*, 31204. (e) Svetlov, A. A.; Sinitsyn, M. N.; Fal'kengof, A. T.; Kokunov, Y. V. *Zh. Neorg. Khim.* **1990**, *35*, 1767; *Chem. Abstr. 114*, 54722. (f) Salomov, A. S.; Mikhailov, Y. N.; Kanishcheva, A. S.; Svetlov, A. A.; Sinitsyn, N. M.; Porai-Koshits, M. A.; Parpiev, N. A. *Zh. Noerg. Khim.* **1988**, *33*, 2608; *Chem. Abstr. 110*, 16418. (g) Sinitsyn, N. M.; Travkin, V. F.; Svetlov, A. A.; Itkina, Z. B. *Koord. Khim.* **1975**, *1*, 103; *Chem. Abstr. 83*, 21193.

(13) (a) Wanner, M.; Scheiring, T.; Kaim, W.; Slep, L. D.; Baraldo, L. M.; Olabe, J. A.; Zalis, S.; Baerends, E. J. *Inorg. Chem.* **2001**, *40*, 5704. (b) Baumann, F.; Kaim, W.; Baraldo, L. M.; Slep, L. D.; Olabe, J. A.; Fiedler, J. *Inorg. Chim. Acta* **1999**, *285*, 129.

(14) Sieger, M.; Sarkar, B.; Zalis, S.; Fiedler, J.; Escola, N.; Doctorovich, F.; Olabe, J. A.; Kaim, W. *J. Chem. Soc., Dalton Trans.* **2004**, 1797.

(15) Callahan, R. W.; Meyer, T. J. *Inorg. Chem.* **1977**, *16*, 574.

The ferrocene/ferrocenium (Fc/Fc^+) couple served as internal reference. Low-temperature measurements were made using the established[16] solvent *n*-PrCN = *n*-butyronitrile. For polarography a PAR 263A potentiostat was used. Spectroelectrochemistry was performed using an optically transparent low-temperature cell.[17a] A two-electrode capillary served to generate intermediates for X band EPR studies.[17b]

Synthesis. The $[Cl_5Os(NO)]^{2-}$ ion was initially obtained as the bis(tetraphenylphosphonium) salt according to the literature.[12a] However, the PPh_4^+ ion is irreversibly reduced around −2.1 V against ferrocenium/ferrocene, in a similar potential range as $[Cl_5Os(NO)]^{2-}$. Therefore, $(n\text{-}Bu_4N)_2[Cl_5Os(NO)]$ was prepared through cation exchange. A solution of 72 mg (0.186 mmol) of $(n\text{-}Bu_4N)PF_6$ in 10 mL of methanol was added to a solution of 100 mg (0.093 mmol) of $(Ph_4P)_2[Cl_5Os(NO)]$ in 20 mL of methanol with constant stirring at room temperature. The mixture was stirred for 1 h at room temperature, and the resulting solid, $(Ph_4P)PF_6$, was separated by filtering the mixture. The light brown filtrate contained the desired compound. A small amount of $(n\text{-}Bu_4N)PF_6$ was added to the filtrate to ensure the complete precipitation of the phosphonium salt and remove any further precipitate. The filtrate was evaporated to dryness, and the gray solid residue was ground with 20 mL of water to remove the excess of $(n\text{-}Bu_4N)PF_6$ which is poorly soluble in water. Evaporating the filtrate to dryness and drying the gray residue in a vacuum yielded 74 mg of the product. Anal. Calcd for $C_{32}H_{72}Cl_5N_3OOs$ (882.40): C, 43.56; H, 8.22; N, 4.76. Found: C, 43.83; H, 8.32; N, 4.50%. Further characterization is described in the main text.

The compound *cis*-$[(bpy)_2ClOs(NO)](PF_6)_2$ was prepared according to the literature.[11]

X-ray Structural Determination of $(PPh_4)_2[Cl_5Os(NO)]\cdot 4CH_3CN$. Brown crystals were grown by recrystallization from acetonitrile. The X-ray intensity data were collected on a Nonius Kappa CCD system. The final unit cell parameters were determined from the least-squares refinement of 52 536 reflections. Intensity data were corrected for absorption by using symmetry-related reflections. The structure was solved by direct methods and refined by employing full-matrix least-squares on F^2 using the SHELTXL program package.[18] All non-hydrogen atoms were refined anisotropically, and hydrogen atoms were included in idealized positions. In the dianion, the axial chlorine atom Cl3 and the nitrosyl group are disordered with respect to an inversion center; they were refined with split positions and occupation factors of 0.50, respectively. Important crystallographic data and final *R* values are listed in Table 1.

Table 1. Crystallographic Data for $(PPh_4)_2[Cl_5Os(NO)]\cdot 4CH_3CN$

empirical formula	$C_{56}H_{52}Cl_5N_5OOsP_2$
fw	1240.42
T (K)	100(2)
λ (Å)	0.71073
cryst syst	monoclinic
space group	$P2_1/c$
Z	2
a (Å)	9.5056(1)
b (Å)	19.4011(2)
c (Å)	14.8581(2)
β (deg)	98.262(6)
V (Å^3)	2711.68(5)
ρ_{calcd} (g cm^{-3})	1.519
μ (mm^{-1})	2.701
θ range (deg)	2.96−28.29
collected data (R_{int})	59472 (0.0602)
unique data/unique data with $I > 2\sigma$	6695/6160
no. of params	359
GOF[a]	1.581
R1, wR2 ($I > 2\sigma$)[b]	0.0183, 0.0536
R1, wR2 (all data)[b]	0.0211, 0.0548

[a] GOF = $\{\sum[w(F_o^2 - F_c^2)^2]/(n-p)\}^{1/2}$, where n and p denote the number of data and parameters. [b] R1 = $\sum(||F_o| - |F_c||)/\sum|F_o|$ and wR2 = $\{\sum[w(F_o^2 - F_c^2)^2]/\sum[w(F_o^2)^2]\}^{1/2}$ where $w = 1/[\sigma^2(F_o^2) + (aP)^2 + bP]$ and $P = [(\max; 0, F_o^2) + 2F_c^2]/3$.

DFT Calculations. Ground-state electronic structure calculations on $[Cl_5Os(NO)]^{n-}$ complexes have been done on the basis of density-functional theory (DFT) methods using the ADF2004.1 [19,20] and Gaussian 03 [21] program packages.

Within the ADF program, Slater type orbital (STO) basis sets of triple-ζ quality with two polarization functions were employed. Basis I was represented by frozen core approximation (1s for N, O, 1s−2p for Cl, and 1s−4d for Os were kept frozen); basis II includes core electrons also. The following density functional was used within ADF: the local density approximation (LDA) with VWN parametrization of electron gas data or the functional including Becke's gradient correction[22] to the local exchange expression in conjunction with Perdew's gradient correction[23] to the LDA expression (ADF/BP). The scalar relativistic (SR) zero order regular approximation (ZORA) was used within ADF calculations. The **g** tensor was obtained from a spin-nonpolarized wave function after incorporating the spin−orbit (SO) coupling. The **A** tensors and the **g** tensor are obtained by first-order perturbation theory from ZORA Hamiltonian in the presence of a time-independent magnetic field.[24,25] Electronic transition energies and compositions were calculated by the asymptotically correct SAOP functional (ADF/SAOP),[28] which is more accurate for higher-lying molecular orbitals and electronic transitions. Core electrons were included in ADF/SAOP calculations.

Within Gaussian 03, Dunning's polarized valence double-ζ basis sets[26] were used for N, O, and Cl atoms and the quasirelativistic effective core pseudopotentials and corresponding optimized set

(16) Fry, A. J., Kissinger, P. T., Heineman, W. R., Eds. *Laboratory Techniques in Electroanalytical Chemistry*, 2nd ed.; Marcel Dekker: New York, 1996; p 469.

(17) (a) Mahabiersing, T.; Luyten, H.; Nieuwendam, R. C.; Hartl, F. *Collect. Czech. Chem. Commun.* **2003**, *68*, 1687. (b) Kaim, W.; Ernst, S.; Kasack, V. *J. Am. Chem. Soc.* **1990**, *112*, 173.

(18) Sheldrick, G. M. *SHELXTL*, version 5.10; Bruker AXS Inc.: Madison, Wisconsin, 1998.

(19) Fonseca Guerra, C.; Snijders, J. G.; Te Velde, G.; Baerends, E. J. *Theor. Chem. Acc.* **1998**, *99*, 391.

(20) van Gisbergen, S. J. A.; Snijders, J. G.; Baerends, E. J. *Comput. Phys. Commun.* **1999**, *118*, 119.

(21) Frisch, M. J.; Trucks, G. W.; Schlegel, H. B.; Scuseria, G. E.; Robb, M. A.; Cheeseman, J. R.; Montgomery, J. A., Jr.; Vreven, T.; Kudin, K. N.; Burant, J. C.; Millam, J. M.; Iyengar, S. S.; Tomasi, J.; Barone, V.; Mennucci, B.; Cossi, M.; Scalmani, G.; Rega, N.; Petersson, G. A.; Nakatsuji, H.; Hada, M.; Ehara, M.; Toyota, K.; Fukuda, R.; Hasegawa, J.; Ishida, M.; Nakajima, T.; Honda, Y.; Kitao, O.; Nakai, H.; Klene, M.; Li, X.; Knox, J. E.; Hratchian, H. P.; Cross, J. B.; Bakken, V.; Adamo, C.; Jaramillo, J.; Gomperts, R.; Stratmann, R. E.; Yazyev, O.; Austin, A. J.; Cammi, R.; Pomelli, C.; Ochterski, J. W.; Ayala, P. Y.; Morokuma, K.; Voth, G. A.; Salvador, P.; Dannenberg, J. J.; Zakrzewski, V. G.; Dapprich, S.; Daniels, A. D.; Strain, M. C.; Farkas, O.; Malick, D. K.; Rabuck, A. D.; Raghavachari, K.; Foresman, J. B.; Ortiz, J. V.; Cui, Q.; Baboul, A. G.; Clifford, S.; Cioslowski, J.; Stefanov, B. B.; Liu, G.; Liashenko, A.; Piskorz, P.; Komaromi, I.; Martin, R. L.; Fox, D. J.; Keith, T.; Al-Laham, M. A.; Peng, C. Y.; Nanayakkara, A.; Challacombe, M.; Gill, P. M. W.; Johnson, B.; Chen, W.; Wong, M. W.; Gonzalez, C.; Pople, J. A. *Gaussian 03*, revision B. 05; Gaussian, Inc.: Wallingford, CT, 2004.

(22) Becke, A. D. *Phys. Rev. A* **1988**, *38*, 3098.

(23) Perdew, J. P. *Phys. Rev. A* **1986**, *33*, 8822.

(24) van Lenthe, E.; van der Avoird, A.; Wormer, P. E. S. *J. Chem. Phys.* **1998**, *108*, 4783.

(25) van Lenthe, E.; van der Avoird, A.; Wormer, P. E. S. *J. Chem. Phys.* **1997**, *107*, 2488.

(26) Woon, D. E.; Dunning, T. H. J. *J. Chem. Phys.* **1993**, *98*, 1358.

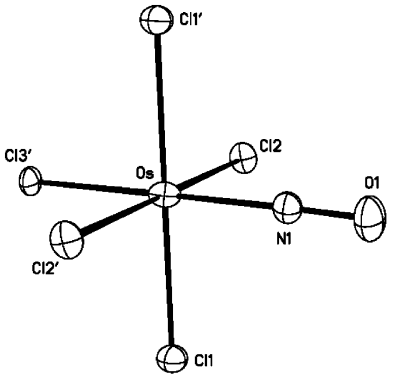

Figure 1. Molecular structure of the dianion in the crystal of $(Ph_4P)_2[Cl_5Os(NO)]\cdot 4CH_3CN$ at 100 K.

Table 2. Selected DFT (ADF/BP) Calculated Bond Lengths (Å) and M−N−O Angles (deg) within $[Cl_5Os(NO)]^{n-}$ Complexes

		$[Cl_5Os(NO)]^{2-}$		
	$[Cl_5Os(NO)]^-$ DFT	DFT	exptl	$[Cl_5Os(NO)]^{3-}$ [a] DFT
M−N	1.759	1.733	1.830(5)	1.808
$M-Cl_{ax}$	2.339	2.392	2.270(1)	2.613
$M-Cl_{eq}$ [b]	2.374	2.444	2.387(4) [b]	2.479 [c] 2.552
N−O	1.170	1.185	1.147(4)	1.246
M−N−O	179.2	180.0	178.5(8)	143.1

[a] Energy minimum (staggered conformation). [b] Average value. [c] Cl_{eq} atoms closer to NO ligand.

of basis functions[27] for Os. The vibrational analysis was done with the "pure" density functional BPW91 [22,29a] and hybrid functional B3LYP.[29b]

The geometries of all complexes were optimized without any symmetry constraints, open shell systems within the spin-unrestricted open shell Kohn−Sham (UKS) approach. As geometry optimizations of $[Cl_5Os(NO)]^{2-}$ lead to approximate C_{4v} symmetry, calculations on this systems were performed in C_{4v} constrained symmetry, the *z* axis coinciding with the C_4 symmetry axis. All results discussed correspond to optimized geometries using the corresponding functional.

Results and Discussion

Crystal Structure. The precursor $(Ph_4P)_2[Cl_5Os(NO)]$ was synthesized as described previously[12a] and characterized additionally by X-ray crystallography (Tables 1 and 2, Figure 1). Although the quality of the structure determination was hampered by disorder, the essential data are compared in Table 2 with DFT calculated values. Table 2 also includes calculation results for the oxidized ($n = 1$) and reduced forms ($n = 3$) of the redox system $[Cl_5Os(NO)]^{n-}$.

Even considering rather high estimated standard deviation (esd) values, the comparison between experiment and calculation reveals significant deviations for the Os−N and Os−Cl bonds, calculated too short and too long, respectively. Like the N−O distance (calculated too long) these results indicate an exaggerated degree of metal−nitrosyl π back-donation by the DFT approach.

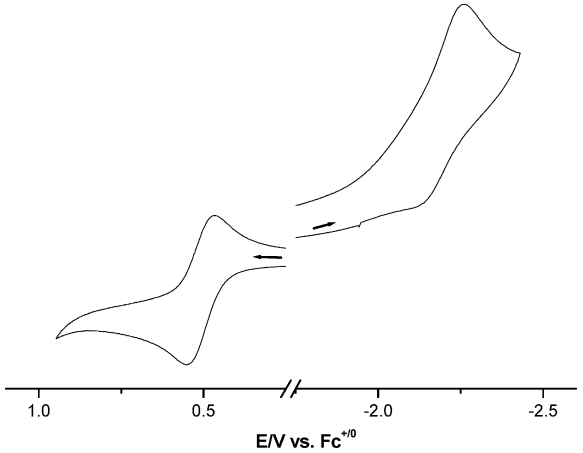

Figure 2. Cyclic voltammograms of $(n\text{-}Bu_4N)_2[Cl_5Os(NO)]$ in *n*-PrCN/0.1 M $n\text{-}Bu_4NPF_6$ at −70 °C (reduction) and 25 °C (oxidation).

Table 3. Redox Potentials[a] of Complexes

complex	$E_{1/2}$ (oxidn)	$E_{1/2}$ (redn)	solvent
$[Cl_5Os(NO)]^{2-}$	0.56 (25 °C) [b]	−2.24 [c] (−70 °C)	*n*-PrCN
$[Cl_5Ru(NO)]^{2-}$	1.02 (−40 °C)	−1.92 [d] (−60 °C)	*n*-PrCN
$[Cl_5Ir(NO)]^-$	>1.5	−0.33 (−60 °C)	*n*-PrCN
$[(CN)_5Os(NO)]^{2-}$	not obsd	−1.50 (25 °C)	CH_3CN [e]

[a] Potentials in V vs $[Fe(C_5H_5)_2]^{+/0}$ from cyclic voltammetry in 0.1 M Bu_4NPF_6 solutions. [b] Corresponding results were obtained for the $^+PPh_4$ salt in acetonitrile (ref 12). [c] Cathodic peak potential for irreversible wave (see text). [d] Peak potential for irreversible process. [e] From ref 13.

Ion Exchange and Cyclic Voltammetry. Since the PPh_4^+ ion is irreversibly reduced around −2.1 V versus $Fc^{+/0}$, in a similar potential range as $[Cl_5Os(NO)]^{2-}$, the $(n\text{-}Bu_4N)_2[Cl_5Os(NO)]$ salt was prepared through ion exchange. It gave essentially identical absorption spectra in the visible and a comparable NO stretching band in the IR spectrum as $(Ph_4P)_2[Cl_5Os(NO)]$.

At −70 °C in *n*-PrCN/0.1 M Bu_4NPF_6 (*n*-PrCN = *n*-butyronitrile) solution the well-soluble $(n\text{-}Bu_4N)_2[Cl_5Os(NO)]$ showed only an irreversible reduction wave, even in the presence of excess Cl^-, in addition to the reversible oxidation[12a,e] (Figure 2). At higher temperatures the reduction becomes completely irreversible because of a faster reaction following the primary one-electron transfer (presumably chloride dissociation, see below). Table 3 lists the potentials in comparison to those of $[Cl_5Ru(NO)]^{n-}$ ($n = 1, 2$), $[Cl_5Ir(NO)]^{n-}$ ($n = 1, 2$), and $[(CN)_5Os(NO)]^{n-}$ ($n = 2, 3$).

Obviously, the osmium system exhibits the lowest oxidation *and* reduction potentials. While it is not unexpected that the $Os^{II/III}$ transition is more facile than $Ru^{II/III}$ or $Ir^{III/IV}$, the very negative potential of the largely NO-based reduction of $[Cl_5Os(NO)]^{2-}$ is quite remarkable. It illustrates the well-known efficient π back-donation from osmium(II),[30] here to the π acceptor NO^+, leading to a particularly high degree of covalency in that $\{OsNO\}^6$ configuration.[2] Covalency and the π donor character of Os^{II} result in a reluctance to accept an electron to yield $NO^\bullet$ or Os^I in the $\{OsNO\}^7$ form $[Cl_5Os(NO)]^{3-}$. As Table 3 shows, this effect is less

(27) Andrae, D.; Haeussermann, U.; Dolg, M.; Stoll, H.; Preuss, H. *Theor. Chim. Acta* **1990**, *77*, 123.
(28) Schipper, P. R. T.; Gritsenko, O. V.; van Gisbergen, S. J. A.; Baerends, E. J. *J. Chem. Phys.* **2000**, *112*, 1344.
(29) (a) Perdew, J. P.; Wang, Y. *Phys. Rev. B: Condens. Matter Mater. Phys.* **1992**, *45*, 13244. (b) Becke, A. D. *J. Chem. Phys.* **1993**, *98*, 5648.
(30) Keane, J. M.; Harman, W. D. *Organometallics* **2005**, *24*, 1786.

Table 4. Calculated Bond Lengthening on Reduction of Complexes $[Cl_5(NO)M]^{n-}$

bond lengthening[a]	M = Ru, $n = 2, 3$	M = Os, $n = 2, 3$	M = Ir, $n = 1, 2$
Δ(M−N)	0.069	0.075	0.099
Δ(M−Cl_{ax})	0.308	0.221	0.145
Δ(N−O)	0.047	0.061	0.045

[a] Bond length differences Δ in Å.

pronounced for the analogous $[(CN)_5Os(NO)]^{2-}$ because five cyanide acceptor ligands compete with one NO^+ for the π donor capacity of osmium(II).

Geometry Changes on Reduction and Oxidation. The lability of both compounds $[Cl_5M(NO)]^{2-}$, M = Ru and Os, on reduction is reflected not only by the negative potentials but also by the calculated lengthening of the bond between M and the axial chloride ligand (trans influence) as shown in Table 2 and as reported previously for ruthenium and iridium analogues (Table 4).[14]

The difference $\Delta(M - Cl_{ax})$ decreases from 0.308 Å for M = Ru via 0.221 Å for M = Os to 0.145 Å for M = Ir. Accordingly, the ruthenium complex could not be reversibly reduced in solution,[14] even at the lowest temperatures, whereas the osmium analogue showed irreversibility at −70 °C and the iridium compound reversible reduction at −40 °C.[14] This labilization of a normally rather inert Os−Cl bond[31] is quite remarkable; it is attributed to strong d(Os)−π*(NO) back-donation and to the trans position. In contrast, the reduction of *cis*-$[(bpy)_2ClOs(NO)]^{2+}$ does not involve chloride labilization, as evident from cyclic voltammetry and polarographic studies.

Table 4 shows a relatively pronounced lengthening of the calculated N−O bond for $[Cl_5Os(NO)]^{2-/3-}$, confirming metal π back-donation into a partially antibonding orbital of the NO• ligand. The calculated lengthening of M−NO distances in the expectedly[2] bent $\{MNO\}^7$ species with nonequivalent M−Cl_{eq} distances and conformational isomerism (cf. Figure 5) increases on going from the ruthenium via the osmium to the iridium compound $[Cl_5Ir(NO)]^{2-}$. The latter also shows a higher degree of bending, calculated at 138.9° and thus lower than the ca. 143° for the ruthenium and osmium systems. Nitrosyl radical complexes with bent metal−NO arrangement can adopt eclipsed or staggered conformations with respect to the coordinated atoms in the equatorial plane (see Figure 5).[7g,8,14] For $[Cl_5Os(NO)]^{3-}$ the staggered structure is favored over the eclipsed one by 0.013 eV = 105 cm^{-1}; the bending angle is calculated slightly larger at 144.1° for the eclipsed conformer.

The oxidized form $[Cl_5Os(NO)]^-$ contains Os^{III} in a linear $\{OsNO\}^5$ configuration. All three states of $[Cl_5Os(NO)]^{n-}$ prefer N-terminal bonded nitrosyl over the NO-side-on bonded alternatives by 1.86 eV ($n = 1$), 1.84 eV ($n = 2$), and 1.69 eV ($n = 3$), respectively.

IR and EPR Spectroelectrochemistry. The apparent accessibility of the oxidized and reduced forms of the $[Cl_5Os(NO)]^{2-}$ ion and of $[(bpy)_2ClOs(NO)]^+$ allowed us to study EPR and IR characteristics by low-temperature spectroelectrochemical techniques.[17] Representative spectra are shown in Figures 3 and 4; Tables 5 and 6 summarize the data together with calculated results. Table 7 lists the calculated spin densities which were the basis for *g* factor calculations.

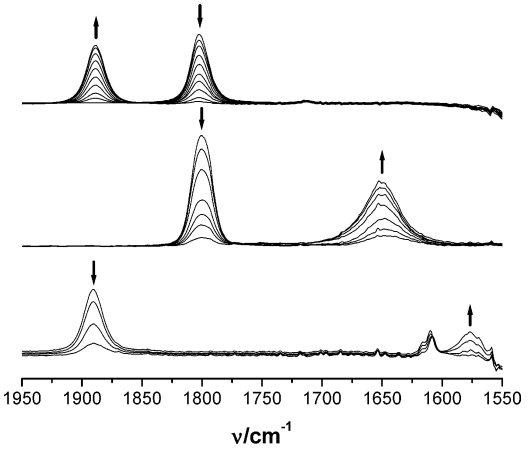

Figure 3. IR spectroelectrochemical response for the oxidation (top, 298 K) and reduction (center, 203 K) of $(n\text{-}Bu_4)[Cl_5Os(NO)]$ in *n*-butyronitrile/0.1 M Bu_4NPF_6 and for the reduction of *cis*-$[(bpy)_2ClOs(NO)](PF_6)_2$ (bottom, 298 K) in CH_3CN/0.1 M n-Bu_4NPF_6.

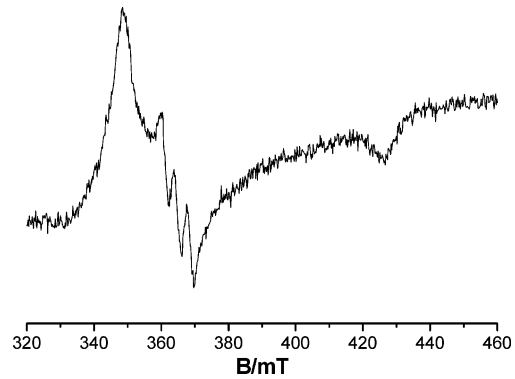

Figure 4. EPR spectrum of reduced *cis*-$[(bpy)_2ClOs(NO)](PF_6)_2$ in CH_3CN/0.1 M n-Bu_4NPF_6 at 4 K: $g_1 = 1.98$, $g_2 = 1.89$, $g_3 = 1.62$, $A_2 = 3.9$ mT.

Table 5. Experimental and G03/BPW91 Calculated NO Stretching Frequencies for $[L_5Os(NO)]^{n-}$ Complexes

	$n = 1$		$n = 2$		$n = 3$	
	calcd ν cm^{-1}	exptl ν cm^{-1}	calcd ν cm^{-1}	exptl ν cm^{-1}	calcd ν cm^{-1}	exptl ν cm^{-1}
$[Cl_5Os(NO)]^{n-}$	1882	1888	1821	1802	1513	*a*
$[(CN)_5Os(NO)]^{n-}$	1902	not obsd	1833	1844[b]	1574	1560[b]

[a] Observed value of 1650 cm^{-1} not believed to be that of $[Cl_5Os(NO)]^{3-}$, see text. [b] From ref 13b.

According to recently reported results for the one-step redox systems $[Cl_5Ru(NO)]^{n-}$ ($n = 1, 2$) and $[Cl_5Ir(NO)]^{n-}$ ($n = 1, 2$),[14] the metal-based oxidation produces a small high-energy shift (≈80 cm^{-1}) of ν(NO) as opposed to a much larger low-energy shift ($\Delta\nu$(NO) = 275 cm^{-1}) for reversible ligand-based reduction.[14] Obviously, the complex $[Cl_5Os(NO)]^{2-}$ shows a mainly metal-based oxidation ($\Delta\nu$(NO) = 86 cm^{-1}; Figure 3, top; Table 5), whereas the irreversible reduction produced a comparatively small shift of only $\Delta\nu$-(NO) = 1802 cm^{-1} − 1650 cm^{-1} = 152 cm^{-1} (Figure 3,

(31) Baumann, F.; Kaim, W.; Denninger, G.; Kümmerer, H.-J.; Fiedler, J. *Organometallics* **2005**, *24*, 1966.

Table 6. Comparison of Experimental and Calculated g Values[a] for $[Cl_5Os(NO)]^-$ and $[Cl_5Os(NO)]^{3-}$ at Optimized Geometry

	$[Cl_5Os(NO)]^-$		$[Cl_5Os(NO)]^{3-}$				
			exptl				
	exptl	calcd	3V[b]	2V[b]	nV[b]	calcd staggered	calcd eclipsed
g_{11}	2.136	2.151	1.998	2.103	2.128	2.122	1.984
g_{22}	2.136	2.149	1.949	1.890	1.864	1.827	1.856
g_{33}	1.998	2.007	1.703	1.638	1.602	1.529	1.604
$g_{11} - g_{33}$	0.138	0.144	0.295	0.465	0.526	0.593	0.380
g_{iso}[c]	2.090	2.102	1.888	1.887	1.877	1.830	1.815

[a] Spin-restricted calculations including spin−orbit coupling (basis I). [b] Species reported from electron trapping in AgCl (ref 6); 3V, 2V, and nV (n = 1 or 0) refer to the number of proximal Ag^+ vacancies. [c] Calculated from $\langle g \rangle = \sqrt{(g_1^2+g_2^2+g_3^2)}/3$.

Table 7. DFT (ADF/BP) Calculated Spin Densities

	$[Cl_5Os(NO)]^-$	$[Cl_5Os(NO)]^{3-}$
M	0.711	0.486
Cl_{eq}[a]	0.098	0.002
Cl_{ax}	0.001	0.038
N	−0.060	0.303
O	−0.045	0.151

[a] Averaged values.

center), incompatible with $[Cl_5Os(NO^{\bullet})]^{3-}$. Support for this assumption comes from the 1844/1560 cm^{-1} reported[13b] for $[(NC)_5Os(NO)]^{2-}/[(NC)_5Os(NO)]^{3-}$ ($\Delta\nu$(NO) = 284 cm^{-1}) or the 1890/1577 cm^{-1} measured for *cis*-$[(bpy)_2ClOs(NO)]^{2+/+}$ ($\Delta\nu$(NO) = 313 cm^{-1}; Figure 3, bottom). In addition, the calculated NO stretching value for $[Cl_5Os(NO)]^{3-}$ is unusually low at 1513 cm^{-1}, that is, more than 150 cm^{-1} lower in comparison to the 1665 cm^{-1} calculated (1677 cm^{-1} experimental) for $[Cl_5Ir(NO)]^{2-}$ and shifted by more than 300 cm^{-1} with respect to the oxidized form $[(Cl_5Os(NO)]^{2-}$. The calculation thus supports the notion of particularly strong d(Os) → π^*(NO) back-donation as evident also from the considerable N−O bond lengthening (Table 4). In consequence, the $\{OsNO\}^7$ configuration appears to involve a significant amount of the $Os^{III}(NO^-)$ formulation[32] in addition to $Os^{II}(NO^{\bullet})$.

To understand the influence of the possible loss of chloride on reduction, calculations on the five-coordinate $[Cl_4Os(NO)]^{2-}$ species and its solvated forms (*n*-butyronitrile modeled by acetonitrile) were done. The optimized structures together with calculated NO stretching frequencies are depicted in Figure S1. The calculations indicate that chloride dissociation shifts the NO frequency to higher wavenumbers; however, the possibility of different closely lying energy minimum configurations is responsible for the remaining ambiguity as to the exact structure of the follow-up product from the reduction of $[Cl_5Os(NO)]^{2-}$.

EPR spectroscopy from low-temperature intra muros electrolysis of $[Cl_5Os(NO)]^{2-}$ supports these interpretations. The reversibly oxidized form $[Cl_5Os(NO)]^-$, also studied previously,[12] can be described as an $Os^{III} = 5d^5$ system with axial splitting of the g components ($g_x > g_y = 2.00$). Individual values, the relatively small g anisotropy Δg, and the average g_{av}, are well reproduced by calculations which include spin−orbit coupling (Table 6). Table 7 shows that the underlying spin density distribution (Os, 0.711) confirms the predominant metal centering of the unpaired electron.

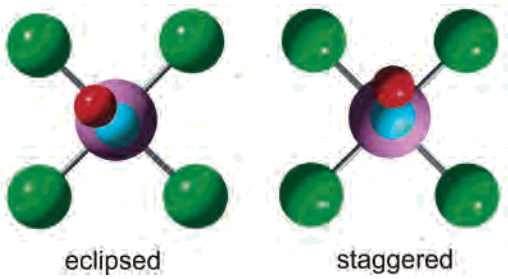

Figure 5. Staggered and eclipsed configurations of $[Cl_5Os(NO)]^{3-}$.

Reduced forms generated from $[Cl_5Os(NO)]^{2-}$ had been analyzed by detailed EPR spectroscopy in AgCl host matrixes where these complexes may serve as (photo)electron traps. Several sets of signals for such species were obtained and assigned to different sites with varying proximal Ag^+ vacancies.[6] After electrolysis at −70 °C in *n*-butyronitrile/0.1 M Bu_4NPF_6, a signal with $g_{\|} = 2.15$ and $g_{\perp} = 2.002$ was observed in frozen solution at 110 K. Such a signal with rather high g components would not be compatible with a $[Cl_5Os(NO)]^{3-}$ structure as suggested by the data from AgCl matrix studies (Table 6) or by the values obtained for $[(NC)_5Os(NO)]^{3-}$ ($g_1 = 1.959$, $g_2 = 1.931$, $g_3 = 1.634$)[13a] or *cis*-$[(bpy)_2ClOs(NO)]^+$ (Figure 4).

Both the IR and EPR spectroelectrochemical studies thus point to an EC process in fluid solution, possibly a dissociation of the chloride in trans position. Calculations reveal that the conceivable products, a pentacoordinate species, a hexacoordinate solvent, or a hydride complex, would exhibit less shifted NO stretching bands and less lowered g components, as similarly shown by Lehnert and co-workers for nitrosyliron compounds.[33] However, at this point the follow-up product of the process cannot be positively identified; the product obtained at low temperature by in situ (IR, EPR) electrochemical reduction undergoes further reactions (decomposition) when the temperature is increased.

We have pointed out before[14] that the very sensitive **g** tensor components are highly dependent on the conformation of the bent NO group in an $\{MNO\}^7$ configuration, that is, in a staggered, eclipsed, or intermediate situation (Figure 5). The staggered conformation of $[Cl_5Os(NO)]^{3-}$ is favored over the eclipsed one by only 105 cm^{-1}; nevertheless, the calculations show significant differences of g components between the conformers (Table 6). Interestingly, the different sets of EPR signals reported[7] for $[Cl_5Os(NO)]^{3-}$ at different sites in AgCl are well reproduced by the ideally staggered (nV, 2V) and eclipsed (3V) conformations, suggesting that these sites induce different conformations and high barriers for rotational interconversion.

For comparison, it should be noted that staggered and eclipsed conformers of nitrosylhemeiron(I) species were calculated to be isoenergetic with the consequence of free rotation around the Fe−(NO) bond.[7g]

(32) Mingos, D. M. P.; Sherman, D. J. *Adv. Inorg. Chem.* **1989**, *34*, 293.

(33) Praneeth, V. K. K.; Neese; F.; Lehnert, N. *Inorg. Chem.* **2005**, *44*, 2570.

Table 8. ADF/SAOP Calculated Compositions (in %) of Frontier Molecular Orbitals of $[Cl_5Os(NO)]^{2-}$, Expressed in Terms of Individual Fragments

	E (eV)	prevailing character	Os	Cl_{eq}	Cl_{ax}	NO
$11b_1$	1.01	Os + Cl	59	41		
22e (LUMO)	0.54	NO + Os	34 (d_{xz}, d_{yz})	3	2	61
$6b_2$ (HOMO)	−1.62	Os + Cl_{eq}	58 (d_{xy})	41		
$2a_2$	−2.59	Cl_{eq}		99		
21e	−2.60	Cl_{eq} + NO + Os	9	77	4	10
20e	−2.93	Cl_{ax}	6	11	71	12
19e	−3.07	Cl_{eq}		99		
$10b_1$	−3.15	Cl_{eq}		99		

Table 9. Selected ADF/SAOP Calculated Lowest Allowed TDDFT Singlet Transitions for $[Cl_5Os(NO)]^{2-}$

	ADF/SAOP			
state	main character (in %)	transition energy[a]	oscillator strength	exptl λ_{max}/ϵ [b]
^1E	99 ($6b_2 \rightarrow 22e$)	2.29 (542)	0.0003	573/48
^1E	99 ($2a_2 \rightarrow 22e$)	3.12 (397)	0.0005	437/71
$^1A_1$	79 (21e → 22e); 17 (20e → 22e)	3.46 (358)	0.008	371/147
$^1A_1$	98 (19e → 22e)	3.59 (345)	0.0005	335/147
^1E	90 ($10b_1 \rightarrow 22e$)	3.67 (337)	0.002	
$^1A_1$	81 ($10b_1 \rightarrow 11b_1$); 13 (20e → 22e)	4.23 (293)	0.025	
$^1A_1$	47 (20e → 22e); 19 ($10b_1 \rightarrow 11b_1$)	4.25 (292)	0.047	

[a] Transition energies in eV (wavelengths in nm). [b] Absorption maxima in nm, molar extinction coefficients in M^{-1} cm^{-1}.

Table 10. Selected ADF/SAOP Calculated Lowest TDDFT Triplet Transitions for $[Cl_5Os(NO)]^{2-}$

state	main character (in %)	transition energy[a]
^3E	99 ($6b_2 \rightarrow 22e$)	2.03 (611)
$^3A_2$	99 ($6b_2 \rightarrow 11b_1$)	2.44 (508)
$^3A_1$	78 (21e → 22e); 19 (20e → 22e)	2.72 (455)
$^3B_1$	93 (21e → 22e)	2.97 (417)

[a] Transition energies in eV (wavelengths in nm).

Orbital Composition and Electronic Transitions. The ADF/SAOP calculated compositions of the frontier orbitals of $[Cl_5Os(NO)]^{2-}$ are listed in Table 8.

The HOMO, $6b_2$, is composed from 58% 5d Os and 41% equatorial 3p Cl orbitals. The doubly degenerate LUMO, 22e, is mainly formed from π^* orbitals of the NO ligand (61%) with 34% contribution from 5d Os. Singlet and triplet transitions were calculated using time-dependent density-functional theory (TDDFT) (Tables 9, 10). The calculated long-wavelength singlet transitions in the visible agree reasonably with the observed absorption bands (Table 9). A remarkable result is the low intensity of these metal-to-ligand charge transfer (MLCT) transitions, confirmed here by TDDFT; this is an aspect which has been noted before for MLCT bands involving π^*(NO) as target orbitals.[11,34]

In contrast, intense d(Os) → π^*(bpy) and π(bpy) → π^*-(bpy) transitions were observed in the UV region (322 and 235 nm) for $[(bpy)_2ClOs(NO)]^{2+}$,[11] as illustrated in Figure 6.

Reduction is expected to result in Os−N−O bending (symmetry lowering) which, together with spin−orbit interactions, causes the originally degenerate e molecular levels to split into nondegenerate ones. As EPR shows, the LUMO is not fully localized at the NO ligand but is distributed also to a significant extent over the central metal atom.

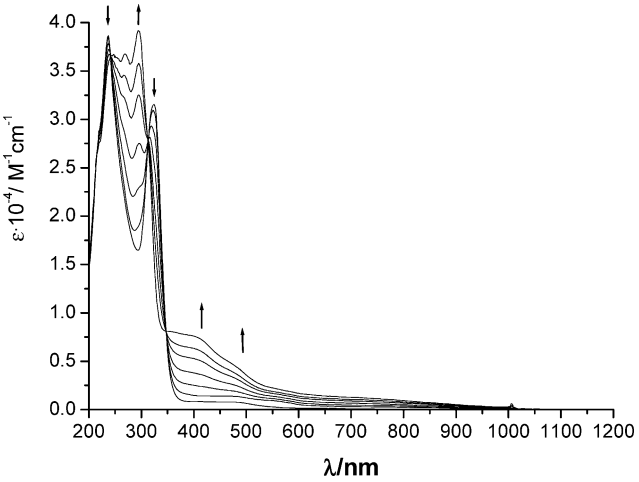

Figure 6. UV−vis spectroelectrochemical response for the conversion $[(bpy)_2ClOs(NO)]^{(2+)\rightarrow(+)}$ in CH_3CN/0.1 M n-Bu_4NPF_6.

The UV−vis spectroelectrochemical reduction experiment for $[(bpy)_2ClOs(NO)]^{2+}$ (Figure 6) shows shifted and split MLCT and intraligand (IL) transitions d(Os) → π^*(bpy) and π(bpy) → π^*(bpy) as intense bands at 294, 269, and 237 nm. In addition, the electrogenerated $[(bpy)_2ClOs(NO)]^{+}$ exhibits several weaker shoulders in the visible region (400, 470, 550br, 680br) which we attribute in part to MLCT transitions d(Os) → π^*(NO•) and to ligand-to-ligand charge-transfer processes π^*(NO•) → π^*(bpy). Transitions involving osmium are generally influenced by the spin−orbit coupling and by considerable ligand contributions due to partial covalent bonding.

In conclusion, this report has demonstrated the applicability of recent experimental and theoretical methodology for the study of relatively simple nitrosylmetal complexes. While basic concepts have been established in this field for quite some time,[2,35] reactive open-shell species containing heavy metals clearly pose considerable challenges. Using two chloronitrosylosmium redox systems, we have investigated the effects of electron transfer in these compounds and the electronic structures of the thus generated species. Remarkably, the pentachloro compound could not be reversibly reduced in fluid solution even at −70 °C despite its established stability in an AgCl matrix. On the other hand, the complex $[(bpy)_2ClOs(NO)]^{+}$ with cis positioned NO• and Cl groups is stable and exhibits EPR features similar to $[(NC)_5Os(NO)]^{3-}$. The good agreement between experimental and DFT computed g factor components supports the confidence in the calculated spin distribution which is estimated at about $^2/_3$ NO centered and $^1/_3$ metal based. These results quantify the notion of significant metal d and π^*-(NO) orbital mixing, justifying the concept of "covalent triatomic MNO species" as expressed by the Enemark−Feltham notation.[2]

(34) Paulat, F.; Kuschel T.; Näther, C.; Praneeth, V. K. K.; Sander, O.; Lehnert, N. *Inorg. Chem.* **2004**, *43*, 6979.

(35) (a) Manoharan, P. T.; Gray, H. B. *J. Am. Chem. Soc.* **1965**, *87*, 3340. (b) Gray, H. B.; Manoharan, P. T.; Pearlman, J.; Riley, R. F. *Chem. Commun.* **1965**, 62.

Acknowledgment. This work has been supported by the Deutsche Forschungsgemeinschaft (graduate college "Magnetic Resonance"), by the European Union (COST D35 action), and by the Grant Agency of the Czech Republic (Grant No. 1ET400400413). We thank Dr. Falk Lissner for the crystallographic data measurements.

Supporting Information Available: X-ray crystallographic file in CIF format for $(Ph_4P)_2[Cl_5Os(NO)]\cdot 4CH_3CN$ and Figure S1 (calculated NO stretching frequencies of possible reduction products from $[Cl_5Os(NO)]^{2-}$). This material is available free of charge via the Internet at http://pubs.acs.org.

IC0517669